Hybrid Analysis of Terahertz Photoconductive Antennas Using Energy Balance Transport Model

Ramin Emadi* , Navid Barani* , As'ad Amirhosseini* and Reza Safian*
*Department of Electrical and Computer Engineering, Isfahan University of Technology, Isfahan, Iran, 84156
Emails: r.emadi@ec.iut.ac.ir, barani.navid@gmail.com, sa.amirhoseyni@ec.iut.ac.ir, rsafian@cc.iut.ac.ir

***Abstract*—A photoconductive antenna with tip-to-tip rectangular electrodes has been numerically investigated in the terahertz (THz) frequency band. Through a hybrid simulation employing an optoelectronic software, Silvaco, and a full-wave electromagnetic solver, CST, we will show that for analysis of photoconductive antennas in high power applications, energy balance transport model compared to the drift-diffusion model become more accurate due to the consideration of diffusion associated with the carriers temperature.**

I. Introduction

A terahertz photoconductive antenna consists of an ultrafast photoconductor such as low temperature-grown GaAs, LTG-GaAs, connected to a terahertz antenna. Pulsed or heterodyned laser illumination of the photoconductor active area generates photocurrent with terahertz frequency components which feed the antenna, producing terahertz radiation.

To analyze terahertz photoconductive antennas and photomixers, drift-diffusion model has been used extensively [1], [2]. However, this model of charge transport neglects non-local transport effects such as velocity overshoot and diffusion associated with the carrier temperature. In high power applications and submicron devices, diffusion associated with the carrier temperature can have a significant effect on the produced photocurrent. To find accurate photocurrent in these applications, energy balance transport model can be regarded as an accurate solution.

II. Modelling and Formulation

Energy balance transport model consists of an additional coupling of the current density to the carrier temperature. The current density expressions from the drift-diffusion model are modified to include this additional physical relationship. This model introduces two new independent variables T_n and T_p, the carrier temperature for electrons and holes, respectively. The electron-hole current densities are then expressed as [3]:

$$\vec{J_n} = qD_n\vec{\nabla}n - q\mu_n n\vec{\nabla}\psi + qnD_n^T\vec{\nabla}T_n \tag{1}$$

$$\vec{J_p} = -qD_p\vec{\nabla}p - q\mu_p p\vec{\nabla}\psi - qpD_p^T\vec{\nabla}T_p \tag{2}$$

where ψ is the electrostatic potential, n is the volume density of electrons and μ_n is the mobility of electrons. D_n is the thermal diffusivity for electrons. Similar definitions also exist for holes [3].

The first and second terms in (1) represent the diffusion current and the drift current, respectively. The drift-diffusion model considers only these two terms. The third term in (1) represents the diffusion associated with the carriers temperature which is the main focus of energy balance transport model. Throughout following sections, we will clarify effect of this phenomenon.

Using simulated photocurrent in Silvaco as a current source for a photoconductive antenna in CST microwave studio, the detected terahertz signal in the receiver side and in frequency domain can be calculated as [4] :

$$J(f) \propto E_{pc}(f)N(f) \tag{3}$$

where $E_{pc}(f)$ is the radiated electric field of transmitter antenna and $N(f)$ is the fourier transform of generated free photo-carrier density in receiver antenna. Here, We have assumed that hypothetically another similar photoconductive antenna operates as a receiver in the far field of the transmitter antenna [4].

III. Simulation Results

Fig.1(a) represents tree dimensional view and dimensions of a photoconductive antenna with tip-to-tip rectangular electrodes. As previously discussed, we have used Silvaco for optoelectronic simulation to calculate accurate excited photocurrent numerically. Moreover, LTG-GaAs is used as a substrate for photoconductive antennas. In Table I, required parameters of this simulation are presented. The proposed structure has the maximum dimension of 10μm. However, to see the effectiveness of energy balance transport model, DC bias is increased to 200V. In Fig.1(b), the profile of the electric potential for this structure is shown. As it can be seen, the electric potential is distributed uniformly around all six electrodes. Fig.2 demonstrates simulated photocurrent for the above structure using both drift-diffusion and energy balance transport model. It is obvious that energy balance transport model results in larger peak value and longer decay time for excited photocurrent compared to the drift-diffusion model.

For the full-wave electromagnetic simulation, we have used CST Microwave Studio. Fig.3 represents the three dimensional view of a dipole photoconductive antenna in CST. Using the simulated photocurrents in the previous part as a current source for the antenna, we calculate the detected terahertz signals of the transmitter antenna in its far field [4]. The resonance frequency of the dipole antenna is assumed to be around $f = 0.2$ THz. For this purpose, the transmitter antenna's

978-1-4799-6591-5/14/$31.00 © 2014 IEEE

Table I
PHYSICAL AND BIAS PARAMETERS OF THE SIMULATED LTG-$GaAs$.

Parameter	Value
Operating temperature	300^ok
Wavelength of laser	$800nm$
Optical power density	$0.4mW/\mu m^2$
Low field electron lifetime	$1ps$
Low field electron mobility	$400cm^2/Vs$
Relative permittivity	13.18
Substrate thickness(T)	$1.5\mu m$
Profile of incident light	Guassian
Laser pulse duration	$60fs$
Voltage bias	$200V$

dimensions are designed to be $L_a = 135$ μm [5], $W = 10$ μm and $G = 5$ μm.

In Fig.4 detected terahertz signal for both drift-diffusion and energy balance transport model are shown. It is obvious that selecting energy balance transport model for analysis of high power applications, can have a great impact on the detected terahertz signal and in fact, is more accurate.

Finally, the validity of all previous simulations is shown in the Fig.5, where a great agreement can be found between the simulation results and the experimental data [6] of a photoconductive antenna with bare gap electrodes for its radiated electromagnetic field in the broadside direction.

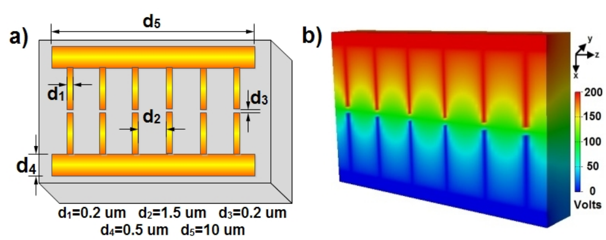

Figure 1. (a): The geometry of a six-finger tip-to-tip rectangular electrodes, (b): The profile of electric potential of this structure.

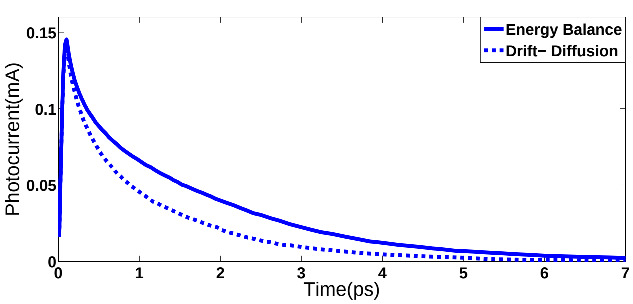

Figure 2. Time-dependent photocurrent for the photoconductive antenna with tip-to-tip electrodes.

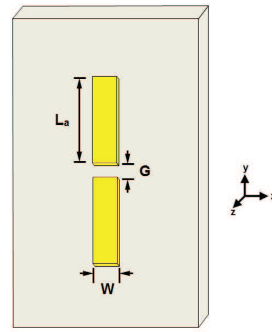

Figure 3. Three dimensional view of a dipole photoconductive antenna in CST.

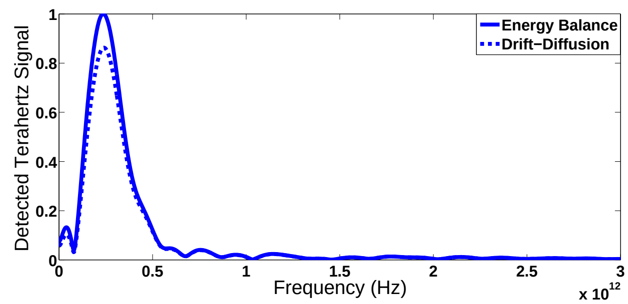

Figure 4. Detected terahertz signal for simulated photocurrents.

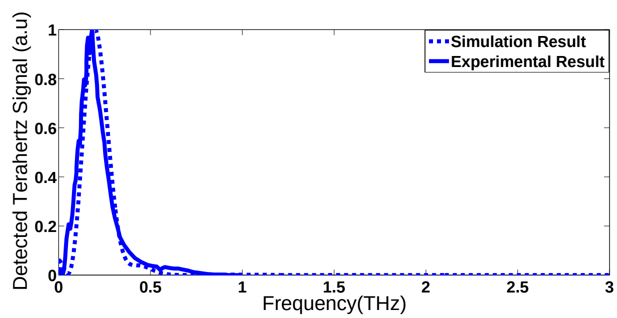

Figure 5. Comparison of simulated and measured detected terahertz signal.

REFERENCES

[1] M. Khabiri, M. Neshat, and S. Safavi-Naeini, "Hybrid computational simulation and study of continuous wave terahertz photomixers," IEEE Trans. on Terahertz Science and Technology, vol. 2, pp. 605-616, 2012.

[2] N. Khiabani, Y. Huang, Y. Shen, and S. Boyes, "Theoretical Modeling of a Photoconductive Antenna in a Terahertz Pulsed System," IEEE Transactions on Antennas and Propagation, vol. 1, pp.1-1, 2013.

[3] ATLAS User's Manual Device Simulation Software, SILVACO, 4701 Patrick Henry Drive, Santa Clara, CA 95054, 2012.

[4] N. Khiabani, Y. Huang, Y. Shen, and S. Boyes, and Q. Xu, "A Novel Simulation Method for THz Photoconductive Antenna Characterization," 7th European Conference on Antennas and Propagation, pp.751-754, 2013.

[5] D. R. Jackson and N. G. Alexopoulos, "Microstrip dipoles on electrically thick substrates," Journal of Infrared and Millimeter Waves," vol.7, No.1, 1986.

[6] M. Tani, K. Yamamoto, E. S. Estacio, C. T. Que, H. Nakajima, M. Hibi, F. Miyamaru, S. Nishizawa and M. Hangyo, "Photoconductive emission and detection of terahertz pulsed radiation usingn semiconductors and semiconductor devices," Journal of Infrared, Millimeter, and Terahertz Waves., vol.33, no. 4, pp. 393–404, 2012.